Convection-Induced Patterns in Phase-Separating Polymeric Fluids

Zdravko Mitov and Eugenia Kumacheva*

Department of Chemistry, University of Toronto, 80 St. George Street, Toronto, Canada M5S 3H6

(Received 9 March 1998)

The process of pattern formation and droplet coarsening has been studied for ternary polymeric fluids in which phase separation was induced by solvent evaporation. For a particular range of solvent evaporation rates and thicknesses of liquid layers, ordered hexagonal patterns were formed at the liquid film-air interface. We ascribe this effect to Bénard-Marangoni convection induced by solvent evaporation and estimate conditions generating periodic two-phase structures in polymeric films. Droplet coarsening rate featured a crossover from $R \sim t^{0.89}$ to $R \sim t^{0.67}$ coinciding with the onset of convection and was explained by convection-induced stabilization of droplets against coalescence. [S0031-9007(98)07184-1]

PACS numbers: 61.25.Hq, 47.54.+r, 61.41.+e, 68.10.–m

Under particular conditions, patterns with a high degree of order and symmetry emerge in phase-separating polymeric fluids on a length scale significantly exceeding molecular dimensions [1,2]. For multicomponent liquids undergoing phase separation due to solvent evaporation, it was suggested that Bénard-Marangoni convection [3] may be a source of ordered patterns. Indeed, cooling of the top surface due to the solvent removal is similar to heating of a fluid film from below in a sense that it generates temperature gradient in a liquid layer. Fluctuations of temperature at the liquid-air interface result in local surface tension variations enhanced by the upward flow of the warmer liquid from the bulk. In a steady state, surface-tension-driven convection arises in the fluid layer.

The manner in which the dynamics of phase separation and structure evolution are influenced by convection has not been studied although it is known that hydrodynamic effects play a significant role in droplet coarsening. For the cooperative action of Brownian motion and hydrodynamic interactions on the domain growth, Siggia [4] showed that hydrodynamic effects accelerate coalescence-induced coarsening to $R \sim t^{l}$, where R is a droplet mean radius, and t is a coarsening time. Furukawa [5], using coupled Navier-Stokes and Cahn-Hillard equations, predicted for 3D systems with a high Reynolds number two new growth modes that originated from a balance of the inertial forces and interfacial tension, i.e., $R \sim t^{n}$ with $n = 1$ and $n = \frac{2}{3}$. Experimental studies of phase-separation dynamics in a gravity-dominated regime showed that flow can either enhance or suppress droplet growth, depending on a balance of viscous and sedimentation forces [6].

It is reasonable to expect that involvement of droplets of a new phase in convection of the intervening liquid would generate coarsening dynamics different from that predicted and observed in a flow-dominated regime.

In Bénard-Marangoni convection, pattern formation is governed by a balance of the surface-tension-driven forces and dissipation due to the thermal diffusion and the frictional action of viscosity [3]. The competition of these factors is expressed by a Marangoni number

$$\mathrm{Ma} = -(\partial\gamma/\partial T)\Delta T d/\nu\rho k\,, \tag{1}$$

where $(\partial\gamma/\partial T)$ is the temperature derivative of the surface tension γ; ΔT is the difference in temperature between the bottom and the top film surfaces; d is the thickness of the fluid layer; ν is the kinematic viscosity, $\nu = \eta/\rho$; ρ, η, and k are the density, the dynamic viscosity, and the thermal diffusivity of the system, respectively. According to the linear stability analysis, the transition to instability occurs at $\mathrm{Ma}_c \approx 80$ [7].

In low-molecular liquids, convection patterns dissipate when heating of the bottom surface or cooling of the top surfaces ceases. In contrast, in polymeric fluids, kinetic limitations, e.g., vitrification, crystallization, and cross-linking coupled to the phase-separation path dramatically reduce the mobility of the system. In this way, nonequilibrium patterns that emerge in the liquid state would be conserved in the solid film. Studies of the "frozen" morphology can shed light on the dynamics of phase separation in fluid systems.

In this work, experiments were performed on fluid polymeric films in which phase separation was caused by the evaporation of a volatile solvent. By controlling solvent evaporation rate and thicknesses of liquid films, we generated convection and examined conditions required for the formation of ordered patterns in phase-separating systems. Another objective was to explore the effect of convection on the coarsening dynamics of a new phase.

Polystyrene (PS, $M_w = 234\,000$) and polymethyl methacrylate (PMMA, $M_w = 306\,000$) were dissolved in toluene at the total polymer concentration 4.1 w%. The weight ratio of PMMA/PS was 1:9. The PMMA molecules were covalently labeled with a fluorescent dye 4-amino-7 nitrobenzo-2-oxa-1,3-diazol (NBD) [8]. The filtered polymer solution was cast onto quartz glass substrates positioned into a sealed chamber. Film thickness d varied from 0.12 to 3 mm and the aspect ratio ranged from 0.05 to 0.002. To control toluene evaporation rate from the films, dry nitrogen was passed through the chamber with a speed varying from (0 to

7.9) $\times 10^{-5}$ m^3/s. Toluene evaporation was monitored by weighing the sample in the chamber at regular time intervals. The duration of experiments was determined by d and the solvent evaporation rate and ranged from 10 to 45 min until a constant film weight was reached. The surface structure of the films, however, developed over a shorter time t, i.e., within 4–25 min after the solution was cast onto the substrate. Further solvent evaporation did not affect the surface morphology of the films. The solvent evaporation rate, m_s, calculated for the linear part of the graph $m_s = f(t)$, varied from 0.23×10^{-3} to 0.72×10^{-3} kg/m^2 s, and showed a minor increase with a thickness of the sample. The difference in temperatures between the top (T_t) and the bottom (T_b) surfaces was measured as $\Delta T = T_b - T_t$ for films with $d > 0.32$ mm by placing two calibrated thermocouples at the liquid-air and liquid-substrate interfaces with an accuracy of ± 0.1 °C. In a steady state, ΔT in films with d in the range from 0.32 to 3 mm varied from 0.4 to 2.5 °C.

The surface and the bulk film structures were studied by laser confocal fluorescent microscopy (LCFM) using a Bio-Rad MRC 600 confocal microscope. The lateral and vertical resolutions were on the order of 0.3 and 0.7 μm, respectively. Images were analyzed by the digital image analysis program IMAGE TOOLS (NIH).

Typical surface structures of the films obtained at different solvent evaporation rates from liquid layers with $d = 0.58 \pm 0.02$ mm are shown in Figs. 1(a)–1(c). An increase in the rate of solvent removal results in the transition from a random distribution of large polydisperse PMMA-rich domains [Fig. 1(a)] to an ordered pattern of PMMA particles arranged mostly in hexagons [Fig. 1(c)]. This change is accompanied by an increase of the number density of the PMMA domains and a reduction of their dimensions.

In the second series of experiments, the thickness d of liquid films was varied while the difference in temperature across films was kept constant. The LCFM micrographs of the surface structure are shown in Figs. 2(a)–2(c). In thin films with $d = 0.22$ mm, a disordered pattern is formed by dimers and trimers of small particles which appeared due to coalescence of small droplets accompanied by the vitrification of the system [Fig. 2(a)]. An increase of d to 0.92 mm generates periodicity of the PMMA domains shown in Fig. 2(b), whereas in layers with $d = 2.5$ mm a chaotic distribution of large polydisperse domains of the PMMA-rich phase is observed.

The experimental observations can be understood in terms of the relationship (1): for a particular solvent, Bénard-Marangoni convection occurs in fluid polymeric layers when the increase of the film thickness and/or solvent evaporation rate (i.e., increase of the latent heat of vaporization) provides the driving force for thermocapillary convection. The hydrodynamic conditions required for the formation of two-phase ordered patterns are estimated in Fig. 3 in which the polydispersity in the interdomain center-to-center distance is plotted as a function

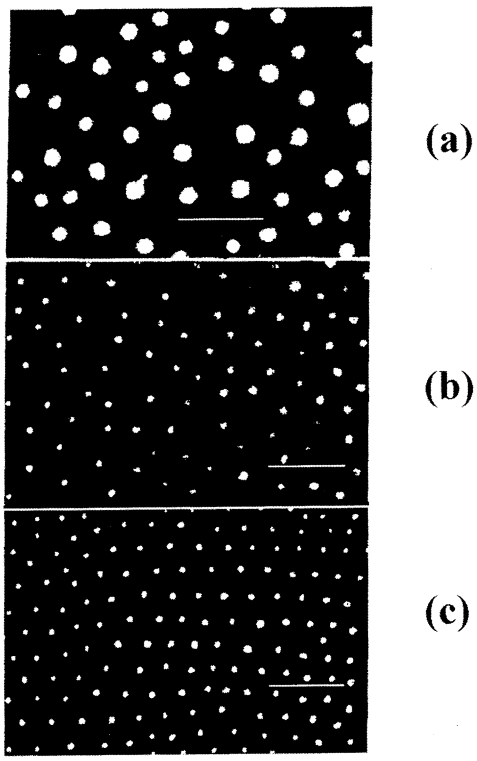

FIG. 1. LCFM images of the surface patterns in PMMA-PS films obtained at different toluene evaporation rates. Fluorescent PMMA-rich domains are prominent on the background of PS. The 488 nm line from an Ar laser was used for the dye excitation. ΔT across the liquid layer: (a) 0.49 °C, (b) 1.05 °C, and (c) 1.51 °C. $d = 0.58 \pm 0.02$ mm. Scale bar is 10 microns.

of the Marangoni number Ma. Polydispersity was defined as $\sigma/\overline{L}$, where σ is the standard deviation of the value of interdomain distance, and $\overline{L}$ is the average interdomain distance. The minimum value in $\sigma/\overline{L} \approx 0.1$ corresponds to the most regular patterns.

A number of assumptions have been made for the calculation of Ma. Rayleigh convection was neglected, since for all liquid layers the ratio Ma/Ra ranged from 11 to 30 where Ra is a Rayleigh number [9]. A variation in the concentration of solvent across liquid films was assumed to be not too large; thus the average composition of liquid layers was used for calculations. Finally, since the concentration of toluene during pattern evolution was bigger than 80 w%, the values of $\partial\gamma/\partial T$, k, and β were assumed to be close to those of the pure solvent. The value of thermal diffusivity was calculated as $k = \alpha/\rho c_p$ [10]. The dynamic viscosity of the intervening liquid was measured as being that of the PS solution at the concentration corresponding to the onset of phase separation [11]. At the concentration of PS in the solution 4.7 w%, the dynamic viscosity was $\eta = 0.09$ P.

The transition to ordered patterns occurs at Ma > 90. In films thicker than 1.8 mm for which Ma exceeds 410, the surface patterns become disordered, presumably due to the turbulence in fluid layers.

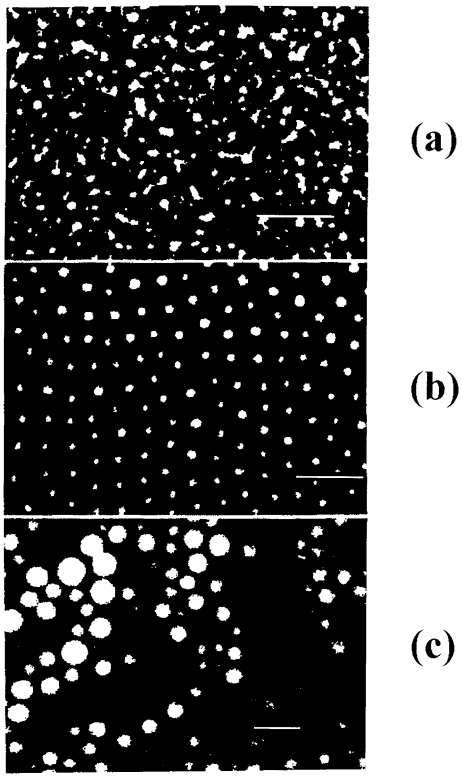

FIG. 2. Surface patterns in blend films formed from PMMA-PS-toluene layers with varying thickness d: (a) $d = 0.32 \pm 0.02$ mm; (b) $d = 0.58 \pm 0.02$ mm; (c) $d = 2.5$ mm. Scale bar is 10 microns.

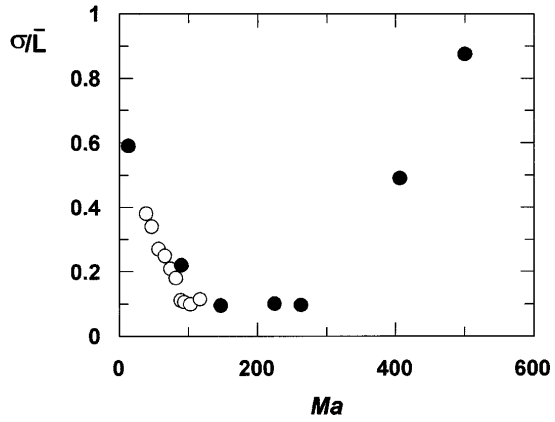

FIG. 3. Standard deviation in the interdomain distance normalized by the average interdomain distance L plotted as a function of a Marangoni number Ma. Ma is controlled by (○) solvent evaporation rate; (●) thickness of the liquid layer.

It has to be noted that surface patterns obtained at $\mathrm{Ma} > \mathrm{Ma}_c$ are not perfectly hexagonal: about 20% of the cells shown in Figs. 1(c) and 2(b) form polygons. Partial distortion can be caused by the nitrogen flow in the chamber. However, more important is the time dependence of the variables in Eq. (1); i.e., $\mathrm{Ma} \equiv \mathrm{Ma}(t)$. The viscosity of the PS-rich solution is the parameter that undergoes the largest change during toluene evaporation, achieving at the moment of a complete pattern formation the value of 0.95 P. This effect implies that for the system studied the Boussinesq-Overbeck approximation [13] is not strictly applicable. In addition, an attachment of PMMA-rich droplets to the air-film interface produces lateral pressure gradients at the horizontal boundary, which compete with those in a z direction. Nevertheless, Fig. 3 demonstrates the approach to producing ordered patterns from phase-separating polymeric systems.

Inspection of the ordered interface patterns reveals that convection cells are ~ 10 μm in size. This value is about 20 times less than expected for liquid films with d ranging from 0.6 to 1.2 mm [3,8]. The reason for the difference may emanate from the occurrence of the convection in a very thin layer adjacent to the free film surface and the non-Newtonian behavior of the intervening fluid.

The dimensions and the number of the PMMA-rich domains are also influenced by hydrodynamic conditions. Figure 4 shows the variation of the mean radius R and the number density n of the PMMA domains as a function of Ma. A crossover in the reduction of R and an increase in n occurs at $\mathrm{Ma} > \mathrm{Ma}_c$; i.e., it coincides with the transition to ordered surface patterns in the corresponding polymeric films. The surface area fraction of PMMA domains is held at 0.087 ± 0.009.

In order to assess more clearly the effect of convection on the rate of coarsening of the PMMA-rich droplets, R was plotted as a function of the coarsening time t (Fig. 5). A short time scale of the experiment made difficult a precise measurement of the power laws of coarsening dynamics. Nevertheless, a crossover in the droplet growth rate was observed at the onset of convection in liquid films: the PMMA-rich domains grew with $R \sim t^{0.89}$ at $\mathrm{Ma} < 90$ and as $R \sim t^{0.67}$ at $\mathrm{Ma} > 90$.

A reduction in the domain growth rate and a stabilization of the particle number density shown in Fig. 4 indicate that (i) at $\mathrm{Ma} < 90$ droplet growth is dominated by coalescence; (ii) when the threshold of convection is exceeded coalescence-induced coarsening is suppressed.

Fast domain coarsening at $\mathrm{Ma} < 90$ can be understood in terms of a cooperation of the Brownian coagulation and flow-dominated coalescence. For near-critical compositions in a flow-dominated regime, Siggia's scaling analysis [4] predicts $n = 1$, a dependence stronger than actually observed. At $\mathrm{Ma} > 90$, the circulation of the intervening liquid between the warmer and cooler spots succeeds the flow occurring between narrow and wide gaps to pressure gradients. Convection-induced stabilization of droplets against coalescence can occur due to the increase of hydrodynamic resistance to the approach of droplets to each other. In these conditions, PMMA-rich droplets are most likely located at warmer sites of the liquid-air interface, i.e., the stagnant spots of the convection cells where circulation of liquid keeps them apart from each other. As a result, droplet growth is dominated by a diffusive process partly supplemented by coalescence with droplets arriving from the bulk of liquid film. In thick liquid films, e.g., Fig. 2(c), the steady state circulation of the PS solution ceases. The

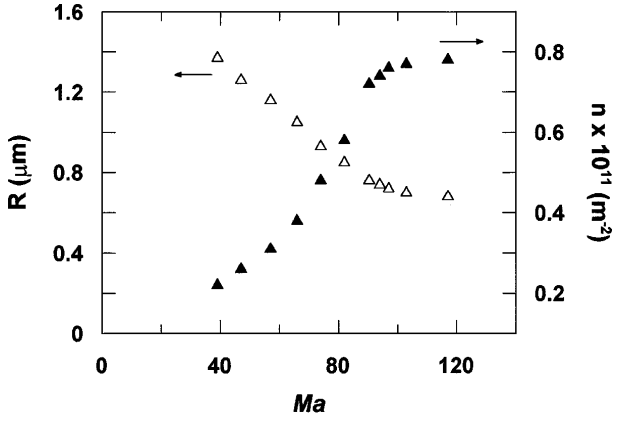

FIG. 4. Plot of the mean radius R (△) and number density n (▲) of the PMMA-rich domains as a function of Ma. $d = 0.58 \pm 0.02$ mm.

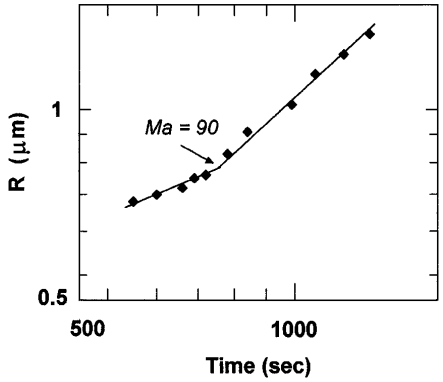

FIG. 5. Average domain radius R of the PMMA phase plotted as a function of coarsening time in liquid PMMA-PS-toluene films with the thickness 0.58 ± 0.02 mm. The shorter time scale corresponds to higher values of Ma.

transition to turbulence accelerates droplet coarsening via coalescence. This effect was predicted by Furukawa [5] for droplet growth at sufficiently high Reynolds numbers.

In films formed from liquid layers at Ma > 90, the layer with a thickness of about 10–20 μm adjacent to the free interface was depleted of PMMA domains. The existence of such layers in corresponding convecting fluids can be anticipated from the droplet drag to warmer spots at the air-liquid interface and toward the hotter film-substrate interface [14]. The velocity of the droplet motion u was estimated as $u = -\{2/[3\eta_L(2\eta_L + 3\eta_D)]\}\{[3\eta_L R/(2 + \chi_D\chi_L)](\partial\gamma/\partial T)\nabla T + (\rho_L - \rho_D)(\eta_L + \eta_D)gR^2\}$ [14], where ∇T is the temperature gradient, χ_L, χ_L, ρ_L and η_D, η_D, ρ_D are the thermal conductivities, viscosities, and densities of the PS-rich solution (intervening liquid) and the PMMA-rich solution in droplets, respectively. Assuming the temperature gradient to be uniform, $\nabla T = (T_b - T_t)/d = 26\,^{\circ}\mathrm{C/cm}$ for the system shown in Fig. 1(c), $\chi_L \approx \chi_D$, $\rho_L \approx \rho_D$, the viscosity of the solution inside and outside the droplets of the order of $\sim 10^{-1}$ P, R of droplets in the bulk solution ~ 0.1 μm, and $\partial\gamma/\partial T = 0.112$ dyne/cm K [11], we obtain the velocity of the droplet motion of about 0.37 μm/s. For the time of pattern formation of about ~ 9 min, the path over which the droplets move would be ~ 200 μm, i.e., 10 times bigger than the thickness of the depleted layer below the top surface. We believe that the difference between the observed and the estimated path is caused by the increase of viscosity of the PS-rich solution due to toluene evaporation.

In conclusion, this is the first experiment that demonstrates the formation of ordered patterns in thin films of phase-separating polymeric liquids by inducing Bénard-Marangnoni convection. We show that by controlling the solvent evaporation rate and the thickness of liquid layers regular surface patterns can be produced in blend films. The onset of the convection occurs at Ma > 90. Convection suppresses droplet coalescence and leads to a crossover in the coarsening rate of the minor phase from $n = 0.89$ to $n = 0.67$ in $R \sim t^n$.

We are grateful to Professor S. Morris for helpful discussions. We thank DuPont Canada, Inc. and NSERC Canada for financial support.

*Electronic address: ekumache@alehemy.chem.utoronto.ca

[1] G. Widawski, M. Rawlso, and B. François, Nature (London) **369**, 387 (1994).
[2] E. Kumacheva, L. Li, M. A. Winnik, D. M. Shinozaki, and P. C. Cheng, Langmuir **13**, 2483 (1997).
[3] R. F. Probstein, *Physicochemical Hydrodynamics* (Butterworths, Boston, 1989), p. 353.
[4] E. D. Siggia, Phys. Rev. A **20**, 595 (1979).
[5] H. Furukawa, Phys. Rev. A **31**, 1103 (1985); **36**, 2288 (1987); Physica (Amsterdam) **204A**, 237 (1994).
[6] F. Cau and S. Lacelle, Phys. Rev. E **47**, 1429 (1993); C. K. Chan and W. I. Goldburg, Phys. Rev. Lett. **58**, 674 (1987); K. W. To and C. K. Chan, Europhys. Lett. **19**, 311 (1992).
[7] J. Pearson, Fluid Mech. **4**, 489 (1958).
[8] S. Sosnowski, J. Feng, and M. A. Winnik, J. Polym. Sci. A, Polym. Chem. **32**, 1497 (1994).
[9] Rayleigh number $\mathrm{Ra} = g\beta\nabla T\, d^3/\nu k$ [2], where g is the gravitational acceleration; β is the liquid expansion coefficient, $\beta = 1.23 \times 10^{-3}\ \mathrm{K}^{-1}$.
[10] The following parameters for the calculation of the thermal diffisivity of toluene were used: thermal conductivity $\alpha = 1.347$ J/cm s K, heat capacity $c_p = 1.69$ J/g K, density $\rho = 0.867$ g/cm^3, and $\partial\gamma/\partial T = 0.112$ dyne/cm K [11].
[11] J. Timmermans, *Physico-Chemical Constants of Pure Organic Compounds* (Elsevier, New York, 1950), Vol. 1, p. 152; J. A. Dean, *Lange's Handbook of Chemistry* (McGraw-Hill, New York, 1992), p. 5.147.
[12] (a) Q. W. Y. Lau and R. Y. M. Huang, J. Appl. Polym. Sci. **29**, 1531 (1984); (b) D. Venegopul and S. Krause, Macromolecules **25**, 4626 (1992).
[13] M G. Velarde and R. Perez Gordon, J. Phys. **37**, 177 (1976).
[14] N. O. Young, J. S. Goldstein, and M. J. Block, J. Fluid Mech. **6**, 350 (1959); J. A. Szymczyk, Appl. Microgravity Tech. II **49**, 49 (1989).